

# Comparing Thermo-Mechanical Anisotropy in Disc-Shaped Specimens: A Case of 3D Printed Silica Sand and Ceramic Sand

S. Ramrattan, L. Wells, and S. Phalke  
Western Michigan University, Kalamazoo, Michigan, USA

Elaine Carlini & Peter Nakachima  
Curimbaba Group, Minas Gerais, Brazil

Copyright 2024 American Foundry Society

## ABSTRACT

Three-dimensional (3D) printing provides the flexibility and ease of producing sand molds directly from computer-aided design (CAD) models. This eliminates the laborious patternmaking steps, thus reducing total production time. Furthermore, 3D printing has additional advantages such as the capability to produce very complex sand cores and molds, affording thinner walls, and requiring no draft.

The purpose of this study is to compare the thermo-mechanical properties of a natural round grain silica sand and a synthetic ceramic sand. The two sands will be 3D printed in separate build boxes to produce disc-shaped specimens. Specimens are processed within a model where binder is applied to sand horizontally and vertically.

The print orientation has a significant effect on longitudinal and radial displacement, and heat transfer properties. This indicates that 3D printed specimens have anisotropic characteristics caused by print orientation, which could result in unanticipated dimensional changes that lead to part rejection. Moreover, there are significant differences in thermal distortion measurements between the natural and synthetic media. Thermal distortion curves showing the anisotropic characteristics between silica and ceramic sands are provided.

**Keywords:** ceramic sand, 3D printing, additive manufacturing, prototyping, rapid casting

## INTRODUCTION

### BACKGROUND

Three-dimensional (3D) printing provides the flexibility and ease of reproducing the sand mold directly from CAD models. This eliminates the laborious patternmaking steps, thus reducing total time to casting.

Where 3D printing provides advantages of minimal processing steps, higher precision and the capability to produce complex-shaped sand molds with thin walls. The use of alternative granular media in 3D printing may provide casting advantages such as superior as-cast surface finish and tighter dimensional tolerance. Thus, the opportunity exists to evaluate and qualify granular media for use in 3D printed molds.

Problems with chemically bonded sand systems arise from variation in materials and processes. There are AFS standard testing procedures for chemically bonded sands using a disc-shaped specimen.<sup>1</sup> With respect to casting quality, the concerns for chemically bonded precision sands and 3D printed sands remain the same.

Despite the industrial health mandate around the use of silica sand, it is still widely used in the foundry industry. The 3D printing of silica sand for additive manufacturing of foundry cores and molds dominates the industry. Furthermore, furan is the predominant chemical binder system being applied when 3D printing cores and molds.

Chemically bonded sand has many potential sources of variation; but it is still subject to the pressures of delivering near-net shaped castings. The sources of variation are grain size, grain shape, chemical composition, binder level, additives, worktime, strip time, pouring temperature, metallostatic pressure, etc.<sup>2</sup> Understanding those variations is a key issue for achieving good process control, and there have been several studies toward that end.<sup>2,3</sup>

The concentration of binder in the sand, and the mix of the binder constituents can all have significant effects on the final castings. Additionally, new binders are constantly being developed in response to various environmental and product quality concerns, thus creating new potential sources of variation.

When sand composites (mold and core media) come in contact with elevated temperature, the heat transferred causes thermo-mechanical movement and thermo-

chemical reactions that result in dimensional changes at the mold-metal interface. At any given temperature these dimensional changes or thermal distortions are attributable to simultaneous changes in both the sand and the binder. Depending on the type of binder used and the temperature at any point in the sand plane, thermally induced reactions occur simultaneously along with sand expansion leading to significant distortions in the composite shape.<sup>3</sup> This paper focuses on understanding the thermal distortions of 3D printed disc-shaped specimens, specifically between different print orientations for silica sand and ceramic sand.

## OBJECTIVES

The objective of this study was to compare a silica sand and a ceramic sand that was 3D printed on the same machine. The effect of binder print orientation on the thermo-mechanical anisotropic properties through thermal distortion of the 3D printed disc-shaped specimen was investigated.

## METHODOLOGY

The methodology consisted of two major steps; preparation of 3D printed disc-shaped specimens and thermal distortion testing. The purpose and procedures for the AFS standardized thermal distortion test are well documented in technical literature.<sup>1,3-7</sup> All specimens were printed at TEI, Livonia, Michigan, USA. Specimens were protected and delivered to Western Michigan University (WMU) in special packaging designed to prevent specimen damage.

*Note:* All specimens were tested in laboratory conditions. Ambient conditions were controlled: temperature at  $20 \pm 1^\circ\text{C}$  ( $68^\circ\text{F} \pm 1.8^\circ\text{F}$ ) and relative humidity at  $50 \pm 2\%$ .

## PREPARATION OF 3D PRINTED SPECIMENS

### Materials and Specimen Processing

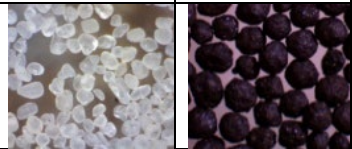
The 3D printed specimens were prepared using washed and dried round grain silica sand and a synthetic ceramic sand. Table 1 describes the raw sands by source, characteristics, chemistry, size, shape, and surface area of the sand grains used in this study.

The silica sand used in this study is conventionally used with a furan binder system for 3D printing of cores and molds in industry. Conversely, the ceramic sand used in this study is new for 3D printing of cores and molds. It is important to point out that 3D printing processing parameters had to be modified to accommodate the coarser and uneven surface of the ceramic sand.

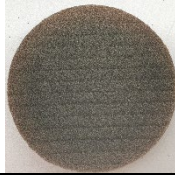
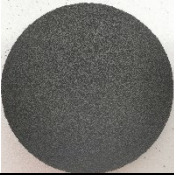
AFS standard disc-shaped specimens (~50 mm dia. ~8 mm thick) were fabricated. The typical 3D printed specimen with sand binder mechanical and physical properties are identified in Table 2.

Noticeably, the ceramic sand specimens were more friable compared to the silica sand specimens.

**Table 1. Typical Properties of the Raw Sands**

| Sand Type:                          | Silica  | Ceramic          |
|-------------------------------------|---|------------------|
| Source                              | IL, USA   | Brazil           |
| Process                             | Natural aggregate   | Sintered Bauxite |
| Chemical Analysis (%)               |   |                  |
| Al <sub>2</sub> O <sub>3</sub>      | 0.07  | 74.0             |
| SiO <sub>2</sub>                    | 99.65   | 6.0              |
| Fe <sub>2</sub> O <sub>3</sub>      | 0.02  | 14.5             |
| TiO <sub>2</sub>                    | 0.01  | 1.8              |
| Other                               | 0.25  | 3.7              |
| USA Sieve No.                       | (% Retained)  |                  |
| 6                                   | 0.00  | 0.00             |
| 12                                  | 0.00  | 0.00             |
| 20                                  | 0.00  | 0.00             |
| 30                                  | 0.00  | 0.00             |
| 40                                  | 0.10  | 0.00             |
| 50                                  | 0.93  | 1.47             |
| 70                                  | 14.22   | 47.84            |
| 100                                 | 55.77   | 45.74            |
| 140                                 | 24.73   | 4.67             |
| 200                                 | 3.87  | 0.28             |
| 270                                 | 0.37  | 0.00             |
| Pan                                 | 0.00  | 0.00             |
| Screens                             | 3   | 2                |
| AFS-GFN                             | 77  | 62               |
| ~Surface Area (cm <sup>2</sup> /g)  | 210   | 164              |
| Bulk Density (g/cm <sup>3</sup> )   | 1.96  | 2.30             |
| LOI (%)                             | 0.085   | <0.01            |
| Fusion/Melt Point (°C)              | 1710  | >1800            |
| pH                                  | 6.9   | 6.8              |
| Acid demand pH-7                    | 1.7   | 1.05             |
| Roundness/<br>Sphericity (Krumbein) | 0.8/0.8   | 0.9/0.9          |
| Shape                               | Rounded   | Round            |
| Surface of Grain                    | Smooth  | Uneven           |
| Color                               | White / Light Tan   | Dark Gray        |
| Grains @ 100X                       |  |                  |

**Table 2. Mechanical and Physical Properties of 3D Printed Disc-shaped Specimens**

| Sand Type             | Silica  | Ceramic   |
|-----------------------|---|---|
| Specimen              |  |  |
| Mass (g)              | 24.07   | 34.66   |
| Impact Strength (J)   | 0.56  | 0.64  |
| Retained Strength (J) | 0.25  | 0.57  |
| Scratch Hardness (#)  | 86  | 70  |
| Abrasion Loss (%)     | 2.43  | 4.24  |
| Permeability (#)      | 193   | 201   |
| LOI Furan Binder (%)  | 1.38  | 1.16  |

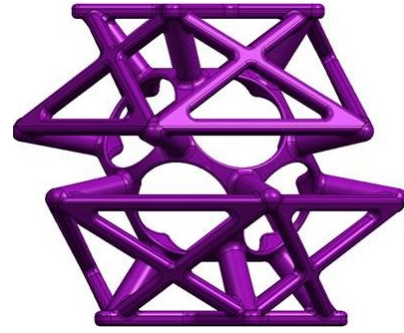


**Figure 2. The custom specimen holder cage structure is shown.**

### Design for 3D Printed Specimens

The specimens, with a diameter of 50mm and height of 8mm, were arranged on the twelve faces of a regular dodecahedron and one was placed in its center. The CAD was developed in Solid Works and is shown in Fig. 1.

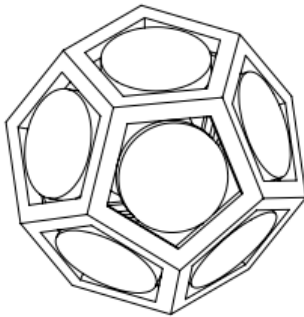


**Figure 1. Cookies arranged in the shape of a dodecahedron in the custom-designed test specimen cage.**

A unique specimen cage was designed around the specimens to protect and secure them in place until they were ready to be tested (Fig. 2). The cage also helped with ease of handling and transportation. Furthermore, the cage had a stand with information related to disc-shaped specimen orientation and coordinate position within the build box (Fig. 3).

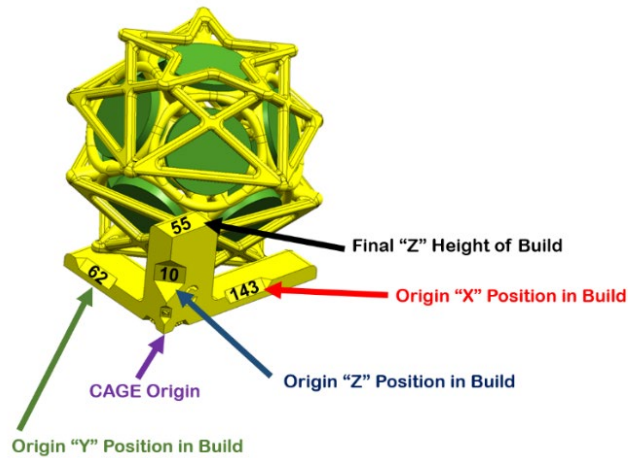


**Figure 3. Cage structure with stand, with specimen orientation and coordinate position printed.**

### 3D Printing

3D printed disc-shaped specimens were produced within the same build box. Processing parameters such as binder level, recoater angle, and print speed were controlled for silica sand production. The printing process parameters were set based on the working condition of producing a 3D printed mold/core for actual castings. The CAD models were positioned at the bottom corner of the build box in the ExOne S-Max Pro 3D sand printer for printing (Fig. 4).



**Figure 4. The ExOne S-Max Pro 3D sand printer build box.**

The recoater drops the sand in the positive y-direction (Fig. 5), and the printhead drops the resin in four passes, alternating in the positive and negative x axis starting from the origin of the build box (Fig. 6).



**Figure 5. Recoater motion direction is shown with arrows.**

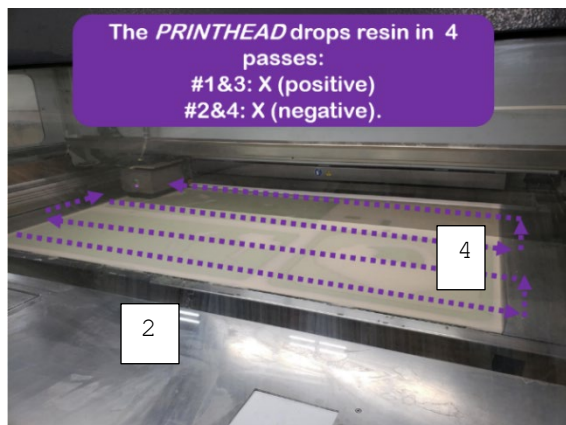


**Figure 6. Printhead motion direction are indicated.**

The build box drops and the recoater and printhead continue making passes until all the parts are printed. The cage structure was printed at the corner of the build box

as it was printed with production which utilized most of the build box volume. The 3D printed parts were removed from the build box by brushing off unbonded sand grains. 3D printed disc-shaped specimens in cage are shown in Fig. 7.

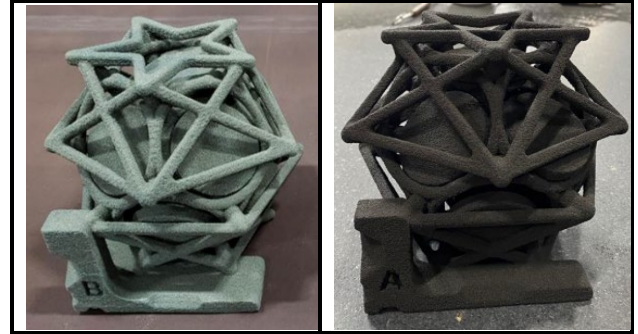


**Figure 7. Printed cages with disc-shape specimens inside the cage, (silica sand on left and ceramic sand on right).**

#### THERMAL DISTORTION TEST

The thermal distortion test was done on the horizontally printed (HP) and vertically printed (VP) disc-shaped specimens. Although not explicitly printed for visibility on the actual disc-shaped specimen, the lines shown in Figs. 8 and 9 indicate the binder orientation for better visualization, but it does not represent the actual binder print specimen. The disc-shaped specimens were subjected to 1000C (1832F) hot surface on the top side, with a head pressure of 4.5N. The longitudinal and radial distortion were recorded and measured.<sup>1, 3-7</sup>



**Figure 8. HP disc-shaped specimen with hot surface (in red). Lines represent binder print orientation.**



**Figure 9. VP disc-shaped specimen with hot surface (in red). Lines represent binder print orientation.**

## RESULTS

The thermal distortion curves (TDC) for longitudinal and radial displacements of the disc-shaped specimens are shown in Fig. 10 through 13. More specifically, Figs. 10 and 11 show the longitudinal displacements for 3D printed silica and ceramic specimens in the HP and VP orientations respectively. Additionally, Figs. 12 and 13 show the radial displacements for 3D printed silica and ceramic specimens in the HP and VP orientations respectively. These TDC's show each specimen type had different outcomes with respect to its longitudinal and radial distortions. Moreover, the sudden upward/downward displacements in the distortion curves for certain disc-shaped specimens indicate crack propagations during testing.

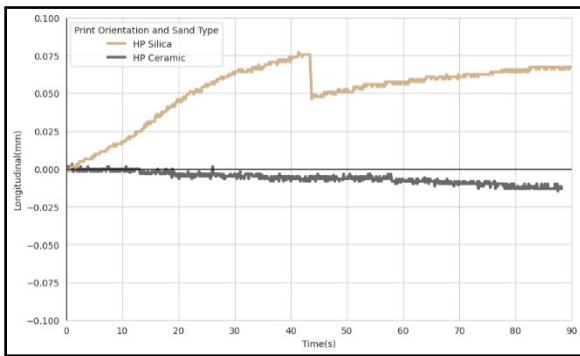


**Figure 10. Longitudinal TDC displacement for horizontally 3D printed silica and ceramic sands.**

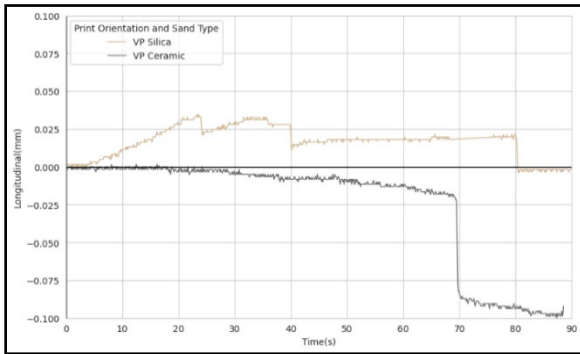


**Figure 11. Longitudinal TDC displacement for vertically 3D printed silica and ceramic sands.**

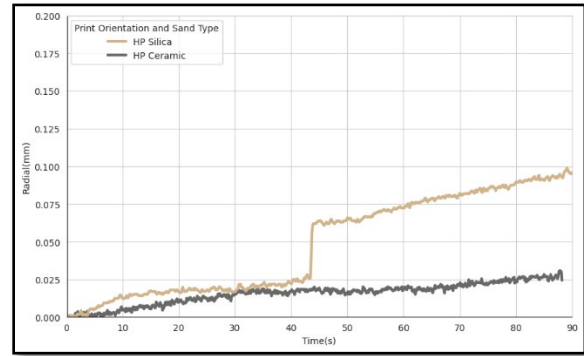


**Figure 12. Radial TDC displacement for horizontally 3D printed silica and ceramic sands.**

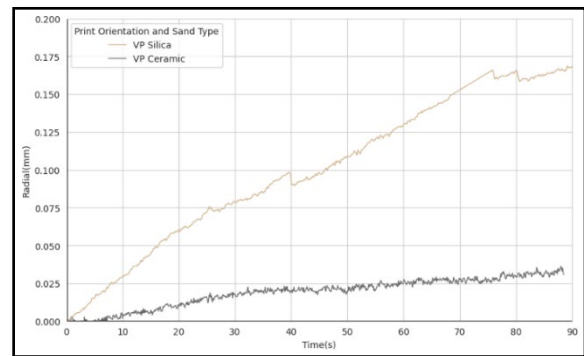


**Figure 13. Radial TDC displacement for vertically 3D printed silica and ceramic sands.**

The TDC's shown in Fig. 10 through 13 are used to calculate total distortion in the sand systems using a numerical integration method.<sup>5,6</sup> The results are shown in Tables 3 and 4. The longitudinal displacement for HP specimens (thicker line width graphs) is generally greater than VP specimens (thinner line width graphs). Interestingly, the radial distortion results are reversed, VP specimens showed greater distortion than HP specimens did. This reveals that within a 3D printed mold, the sand binder tend to expand perpendicularly to its binder print orientation. This is logical since there is more binder in the VP direction.

It is important to point out that thermal distortion was always lower with the 3D printed ceramic specimens. Furthermore, the 3D printed ceramic specimens in the HP direction never cracked during thermal distortion testing. However, the silica sand specimens showed less percent change in mass compared to the ceramic sand specimens (Tables 3 and 4) due to lower resin amount used for 3D printing.



**Table 3. 3D Printed Silica Sand Thermal Distortion Based on Different Print Orientation**

| Silica Sand Specimens | 1000°C TDT @ 4.5 N for 90 seconds   |                               |                              | Observation During Elevated Temp. Testing |                      |
|-----------------------|-------------------------------------|-------------------------------|------------------------------|---|----------------------|
|                       | $D_L$                               | $D_R$                         | $T_D$                        | % Change in Mass                          | Cracks and Fractures |
|                       | Longitudinal Distortion<br>(mm*sec) | Radial Distortion<br>(mm*sec) | Total Distortion<br>(mm*sec) |   |                      |
| HP                    | 4.70                                | 4.40                          | 9.10                         | 1.63                                      | Present              |
| VP                    | 1.56                                | 9.05                          | 10.61                        | 1.86                                      | Present              |

**Table 4. 3D Printed Ceramic Sand Thermal Distortion Based on Different Print Orientation**

| Ceramic Sand Specimens | 1000°C TDT @ 4.5 N for 90 seconds   |                               |                              | Observation During Elevated Temp. Testing |                      |
|------------------------|-------------------------------------|-------------------------------|------------------------------|---|----------------------|
|                        | $D_L$                               | $D_R$                         | $T_D$                        | % Change in Mass                          | Cracks and Fractures |
|                        | Longitudinal Distortion<br>(mm*sec) | Radial Distortion<br>(mm*sec) | Total Distortion<br>(mm*sec) |   |                      |
| HP                     | 0.53                                | 1.38                          | 1.91                         | 2.18                                      | None                 |
| VP                     | 2.21                                | 1.67                          | 3.88                         | 2.02                                      | Present              |

Figures 14 and 15 show the backside temperature for 3D printed silica and ceramic specimens in the HP and VP orientations respectively. The silica sand showed temperature change from beginning to end of test that was 5°C (9°F) for HP and 10°C (18°F) for VP specimens respectively. This indicates that there is more heat transfer in the VP silica sand specimens. The ceramic sand showed temperature change from beginning to end of test that was 4°C (7.2°F) for HP and 3°C (5.4°F) for VP specimens respectively. There is little heat transfer in the ceramic sand specimens. The silica and ceramic sand specimens were both insulating with lower thermal conductivity for the ceramic sand.

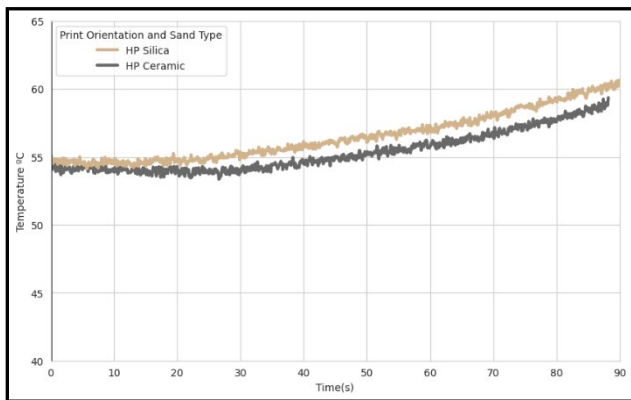


**Figure 14. Temperatures on the back of horizontally 3D printed silica and ceramic sands.**

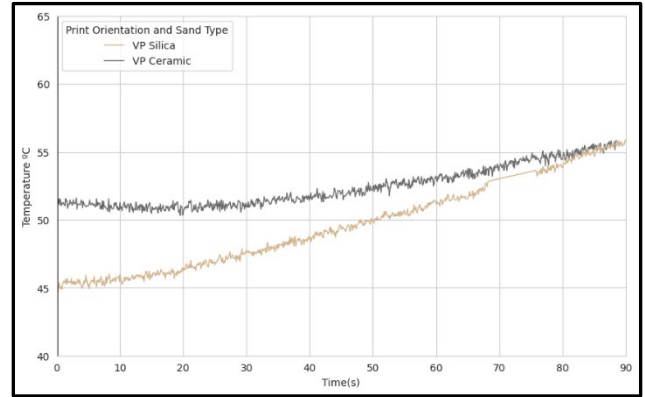


**Figure 15. Temperatures on the back of vertically 3D printed silica and ceramic sands.**

The results show the binder print orientation causes significant differences in terms of the thermally induced distortions both longitudinal and radial directions for both silica and ceramic sand specimens. This indicates that there is thermo-mechanical anisotropy within the same mold, causing unwanted dimensional variations that may cause casting issues due to mold/core wall movement. In conventional chemically bonded sand process (hot-box, cold-box, and no-bake) the sand systems are molded in a homogenous manner. This makes the anisotropic characteristic (VP and HP) unique to 3D printed molds/cores.

## LIMITATIONS

This study was focused on 3D printing utilizing two different sand types and one specific binder system at a set temperature and head pressure representative of a medium sized iron casting. Furan was the only sand binder system employed in this study.

## CONCLUSION AND RECOMMENDATIONS

The application of 3D printed molds and cores presents unique challenges compared to conventional chemically bonded sand systems used in the foundry industry. In this study, the AFS standard disc-shaped specimens were designed and positioned in the faces of a dodecahedron within a cage and coordinate number showing its position. Thermal distortion tests were conducted on the HP and VP printed specimens for silica and ceramic sands.

The results show the binder print orientation has an effect on thermal distortion and heat transfer. Thermal distortion was always greater in the VP direction regardless sand type. Ultimately, issues of mold/core distortion can have an effect on casting surface quality. The 3D printed ceramic specimens in the HP direction was more thermally stable and indicated no crack tendencies during thermal distortion testing when compared to silica sand.

The only concern with the 3D printed ceramic sand is friability and there was a significant percent change in mass occurring at the specimen-hot surface interface.

To understand thermo-mechanical anisotropy in 3D printed sands, a more comprehensive study of print orientation, binder amount, sand type, sand size, and sand distribution is recommended. Testing at actual superheat temperatures for a casting alloy would be more indicative of losses and cracks at specimen hot-surface interface. Furthermore, it recommended that additional 3D printing sand binder systems be studied to reduce friability in the 3D printed ceramic sands.

## ACKNOWLEDGMENTS

The authors gratefully acknowledge Mr. Ted Kahaian, TEI, Livonia, MI for his input on an experimental design and for printing specimens used in this study.

## REFERENCES

1. American Foundry Society Test Procedures for Chemically Bonded Sands, "Mold and Core Test Handbook," 5th. ed., Schaumburg, Illinois, USA (2020).
2. American Society for Metals (ASM), "Metals Handbook, Casting" ISBN: 978-0-87170-711-6, vol. 15 (2008).
3. Iyer, R., Ramrattan, S., Lannutti, J., Li, W., "Thermo-Mechanical Properties of Chemically Bonded Sands," *AFS Transactions*, vol 109, pp. 1-9 (2001).
4. Oman, A. J., Ramrattan, S.N., Keil, M.J., "Next Generation Thermal Distortion Tester," *AFS Transactions*, No. 13-1454 (2013).
5. Ramrattan, S., Patel, P., Shah, R., Senish, T., and Nastac, M., "Non-Standard Testing to Qualify 3D Printed Sands," *AFS Transactions*, No. 16-066 (2016).
6. Ramrattan, S., Wells, L., Patel, P., and Shoemaker, J., "Qualification of chemically bonded sand systems using a casting trial for quantifying interfacial defects," *International Journal of Metalcasting* 12, no. 2, pp. 214-223 (2018).
7. Foo, J., Wells, L., Ramrattan, S., and Tuttle, R., "Considering the Effects of Thermo-Mechanical Anisotropy in 3D Printed Silica Sand Molds," *AFS Transactions*, No. 23-045 (2023).